

The Potential of Gold Nanorods for Larvicidal and Pupicidal Activity Against the Dengue Vector *Aedes Aegypti*

Nur Liyana Razali^{1,2}, Marlia Morsin^{1,2*}, Rahmat Sanudin^{1,2}, Nur Zehan An'nisa Md Shah³, Suratun Nafisah⁴

¹ Microelectronics & Nanotechnology-Shamsuddin Research Centre (MiNT-SRC), Institute for Integrated Engineering, Universiti Tun Hussein Onn Malaysia, 86400, Parit Raja, Batu Pahat, Johor, MALAYSIA

² Department of Electronics Engineering, Faculty of Electrical and Electronic Engineering, Universiti Tun Hussein Onn Malaysia, 86400, Parit Raja, Batu Pahat, Johor, MALAYSIA

³ Sunlight Electrical Pte Ltd, Chin Bee Road, 618679, Jurong, SINGAPORE

⁴ Department of Electrical Engineering, Institut Teknologi Sumatera (ITERA), Lampung Selatan, 35365, INDONESIA

*Corresponding Author: marlia@uthm.edu.my

DOI: <https://doi.org/10.30880/ijie.2025.17.06.019>

Article Info

Received: 30 May 2025

Accepted: 13 September 2025

Available online: 30 December 2025

Keywords

Gold nanorods, larviciding, pupiciding

Abstract

Dengue is an endemic disease in tropical areas, and it is an arthropod-borne viral infection mainly transmitted through an *Aedes* mosquito bite. Due to a rise in dengue transmission in urban and semi-urban regions worldwide, the disease has recently become a significant public health concern, and efficient vector control methods are required. In this study, we proposed the seed-mediated growth method of gold nanorods (GNRs) as a novel and effective tool against the I-IV larval instar and pupae of the dengue vector *Aedes aegypti*. GNRs have an average length of 72.80 ± 0.53 nm and a width of 16.17 ± 0.19 nm. The surface density of GNRs at 20 hours of growth aging period is 76.17 ± 1.98 % with a 3.94 ± 0.33 aspect ratio. The treatment was conducted on 25 larvae/cup in 100 ml of dechlorinated tap water. The larvae start to die after 48 hours. The mortality rates of larvae after 48, 72, 96, and 120 hours, exposed to GNRs are 10.7 ± 0.6 , 24.0 ± 1.0 , 34.7 ± 0.6 and 48.0 ± 1.0 % respectively. Meanwhile, for pupae, the observation shows no dead pupae after 120 hours but for a longer period, several pupae die. The survived pupae are transformed into adult mosquitoes. In conclusion, gold nanoparticles with rod shape (GNRs) have great potential as larvae and pupae treatments for the dengue vector *Aedes aegypti*.

1. Introduction

Dengue fever has become a growing global health concern, with its prevalence increasing significantly since the 1940s due to rapid urbanization, population expansion, international travel, poor sanitation, and inadequate mosquito control measures [1], [2]. The disease has spread across various regions, including the Pacific Islands, the Middle East, and Southeast Asia, placing nearly 40% of the world's population at risk [3]. The dengue virus is primarily transmitted through the bite of female *Aedes aegypti* mosquitoes, which acquire the virus after feeding on infected individuals [4]. Once infected, these mosquitoes continue to spread the virus throughout their lifespan [5].

This is an open access article under the CC BY-NC-SA 4.0 license.



The *Aedes aegypti* mosquito has a complex life cycle comprising aquatic stages (egg and larvae) and terrestrial stages (pupae and adult mosquito). These mosquitoes lay their eggs in stagnant water sources such as containers, discarded materials, and other water-retaining objects. The eggs are highly resilient, capable of surviving in dry environments for extended periods, and they hatch when exposed to water. With each reproductive cycle, females lay multiple batches of eggs, accelerating population growth and increasing the risk of dengue outbreaks, particularly in densely populated areas with favorable environmental conditions.

Mosquito control strategies typically involve biological and chemical approaches. Biological methods, such as introducing natural predators (e.g., fish) or microbial agents (*Bacillus thuringiensis israelensis* and *Bacillus sphaericus*) [6], [7], offer environmentally safe alternatives with minimal resistance development [8]. Chemical methods, such as insecticide fogging and larvicidal agents like temephos, are widely used but have led to resistance in mosquito populations, reducing their long-term effectiveness [9], [10].

With increasing resistance to chemical insecticides, nanotechnology-based solutions have gained attention for vector control [11]. Biosynthesized silver nanoparticles (AgNPs) [6], [12] have effectively killed larvae, but gold nanoparticles (GNPs) offer advantages such as more outstanding biocompatibility, stability, and enhanced chemical properties. GNPs are widely used in biomedical applications, including biosensing and targeted drug delivery, and recent studies have explored their potential as mosquito control agents [13], [14]. Thus far, GNPs are widely used in plasmonic sensors such as pesticide and herbicide detection due to their fast response and high sensitivity [15], [16]. However, most existing research has focused on spherical GNPs.

This study introduces gold nanorods (GNRs) as a promising alternative for controlling *Aedes aegypti* populations by targeting both larvae and pupae. We assess the efficacy of GNRs in terms of mortality rates and lethal concentrations to evaluate their potential as a novel and effective mosquito control strategy.

2. Materials and Methods

The materials and methods for synthesizing GNRs with their characterization are described in detail. Additionally, the larviciding and pupiciding processes are explained.

2.1 Materials

The synthesis of GNRs required several key chemical reagents. Gold (III) chloride trihydrate ($\text{HAuCl}_4 \cdot 3\text{H}_2\text{O}$), sodium borohydride (NaBH_4), hexadecyltrimethylammonium bromide (CTAB), and ascorbic acid ($\text{C}_6\text{H}_8\text{O}_6$) were sourced from Sigma Aldrich, USA. Silver nitrate (AgNO_3) was procured from Honeywell Fluka, US, while hydrochloric acid (HCl) was obtained from RCI Labscan.

2.2 Synthesis of GNRs

All GNRs were synthesized using a seed-mediated growth method (SMGM), involving two main steps: preparing a seed solution and developing the nanorods in a growth solution [17].

For the seed solution, 5 ml of 0.5 mM $\text{HAuCl}_4 \cdot 3\text{H}_2\text{O}$ was combined with 5 ml of 0.2 M CTAB, followed by 0.6 ml of freshly prepared 0.01 M NaBH_4 (Fig. 1), which was kept on ice to maintain its reducing properties. The mixture was allowed to stand undisturbed at 25°C for two hours.

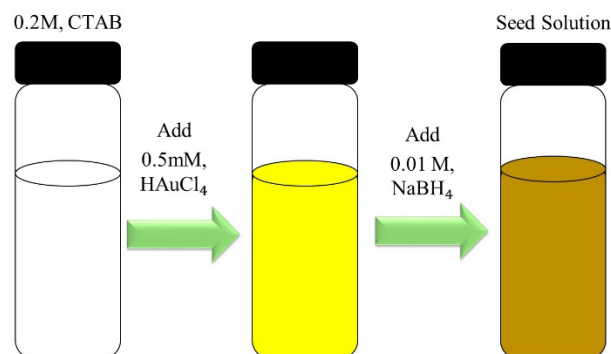


Fig. 1 The seeding process for GNRs

Simultaneously, the growth solution (Fig. 2) was prepared by mixing 15 ml of 1 mM $\text{HAuCl}_4 \cdot 3\text{H}_2\text{O}$ with 15 ml of 0.2 M CTAB. To this, 0.6 ml of 4 mM AgNO_3 and 0.21 μl of 0.0788 M ascorbic acid were introduced. Finally, 0.216 ml of the previously prepared seed solution was added to the growth solution, which was left undisturbed at 25°C for another two hours to promote nanorods formation.

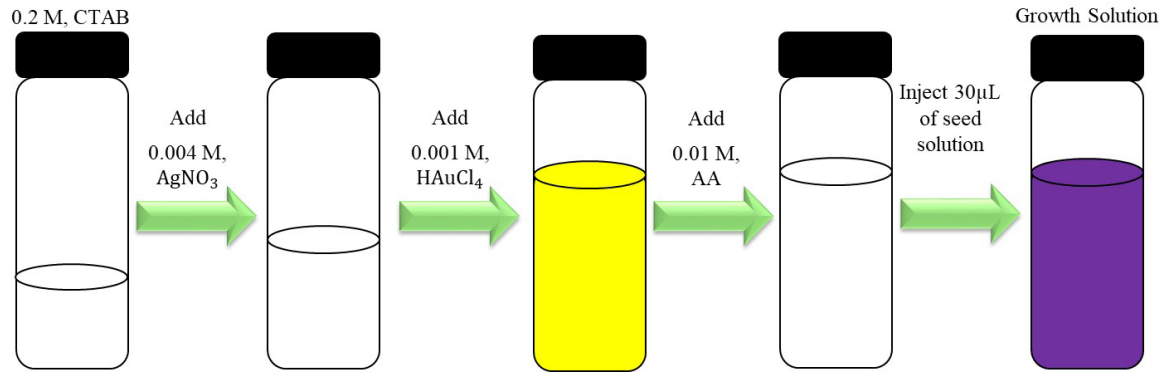


Fig. 2 The growth process for GNRs

2.3 Characterization of GNRs

A series of characterization techniques was employed to analyze the synthesized GNRs. The visual inspection was done by observing the changes in solution color during the synthesis process to monitor the progression of nanoparticle formation. The morphological analysis was done using Field Emission Scanning Electron Microscopy (FESEM) (Model: JSM-7600F, JEOL, Germany) used under a high vacuum at an accelerating voltage of 5 kV to examine the shape and surface structure of the GNRs. Meanwhile, the High-Resolution Transmission Electron Microscopy (HR-TEM) was conducted using a JEOL JEM-ARM200F (Japan) microscope to verify particle size and structural integrity. The spectroscopic analysis was done using UV-visible optical absorption spectroscopy with a Shimadzu UV-1800 spectrophotometer (Japan) to record the optical absorption spectrum of GNRs in the wavelength range of 400–800 nm. Lastly, the crystallographic characterization was performed using X-ray diffraction (XRD) analysis using a PANalytical X'Pert Powder Diffractometer (Netherlands) with $\text{CuK}\alpha$ radiation ($\lambda = 0.1540 \text{ nm}$) and a step size of 0.03° to determine the crystalline properties of the synthesized GNRs.

2.4 Larvicidal and Pupicidal Treatment Using GNRs

The larvicidal and pupicidal potential of GNRs was assessed using laboratory-reared *Aedes aegypti* larvae and pupae provided by the Johor Bahru District Health Office.

For the bioassay, twenty-five-fourth instar larvae were placed in 200 ml paper cups, each containing 100 ml dechlorinated water. The experimental setup for both larviciding and pupiciding is shown in Fig. 3. To evaluate the effectiveness of GNRs, 1 ml of the nanoparticle solution was added to the water. Throughout the experiment, the larvae were provided with food [18], [19].

The study was conducted under controlled environmental conditions, maintaining a temperature of $27 \pm 2^\circ\text{C}$ and relative humidity of $70 \pm 10\%$. A control group was maintained, where larvae were provided food but not exposed to GNRs. Mortality was recorded daily, and dead larvae and pupae were removed regularly to prevent contamination [20], [21].

Mortality rates were adjusted using Abbott's correction formula (1925) to account for natural deaths in the control group [22]:

$$\text{Percentage mortality} = \frac{\text{Number of dead larvae or pupae}}{\text{Number of larvae or pupae introduced}} \times 100 \quad (1)$$



Fig. 3 The experimental setup for both larviciding and pupiciding

3. Results and Discussion

The properties of synthesized GNRs and the result after larvae and pupae treatment using GNRs are discussed.

3.1 Properties of GNRs

The synthesis of GNRs using the seed-mediated growth method (SMGM) was successfully achieved, as confirmed through a series of characterization techniques. Fig. 4 shows the 3D model of GNRs, final solution color after growth process of GNRs and morphological properties of GNRs. One of the initial indicators of successful synthesis was the color change observed during the process. At the nanoscale, color variation provides insights into particle formation, density, size, and shape. After the seeding stage, the solution exhibited a brown hue, indicating the initial formation of gold seeds. As the growth process progressed over 20 hours, the solution gradually turned a darker violet, signifying the formation of uniform GNRs.

FESEM images further verified the successful growth of nanorods. The analysis revealed a rod-like morphology with an average length of 72.80 ± 0.53 nm and a width of 16.17 ± 0.19 nm. The surface density of GNRs after 20 hours of aging reached 76.17%, with an aspect ratio of 3.94 ± 0.33 .

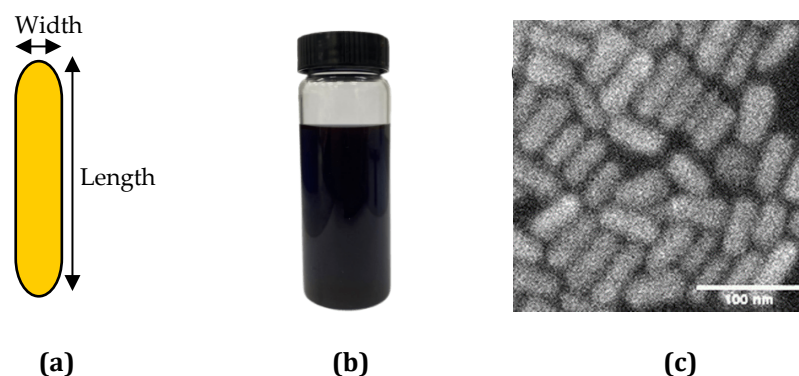


Fig. 4 (a) 3D model of GNRs; (b) final solution color after growth process of GNRs; (c) morphological properties of GNRs

Further structural and morphological analysis using HR-TEM confirmed the nanorod shape at the atomic level (Fig. 5). The lattice fringes observed in HR-TEM images were aligned with the growth axis, with a measured spacing of 0.2008 nm, corresponding to the (200) crystal facets. Additionally, the fast Fourier transform (FFT) pattern confirmed the crystalline nature of the synthesized GNRs.

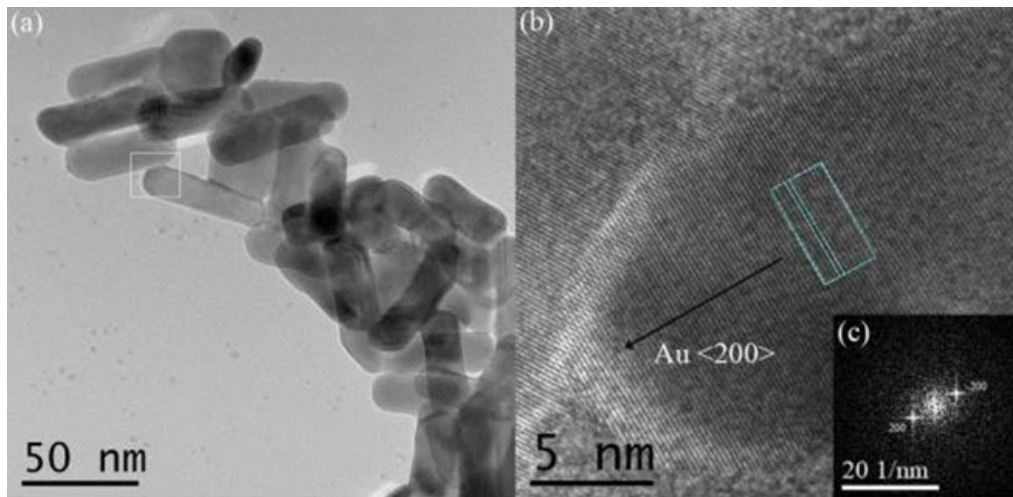


Fig. 5 (a) TEM; and (b) HR-TEM images of GNRs

The XRD, UV-Vis and FTIR results are shown in Fig. 6. XRD analysis was conducted to determine the structural properties of the synthesized GNRs. The diffraction pattern exhibited prominent peaks at $2\theta = 38.2^\circ$ and $2\theta = 44.5^\circ$, corresponding to the (111) and (200) planes, respectively. These diffraction peaks matched the standard reference for gold (ICSD file No. 98-061-1625), confirming the formation of a face-centered cubic (FCC) crystalline structure.

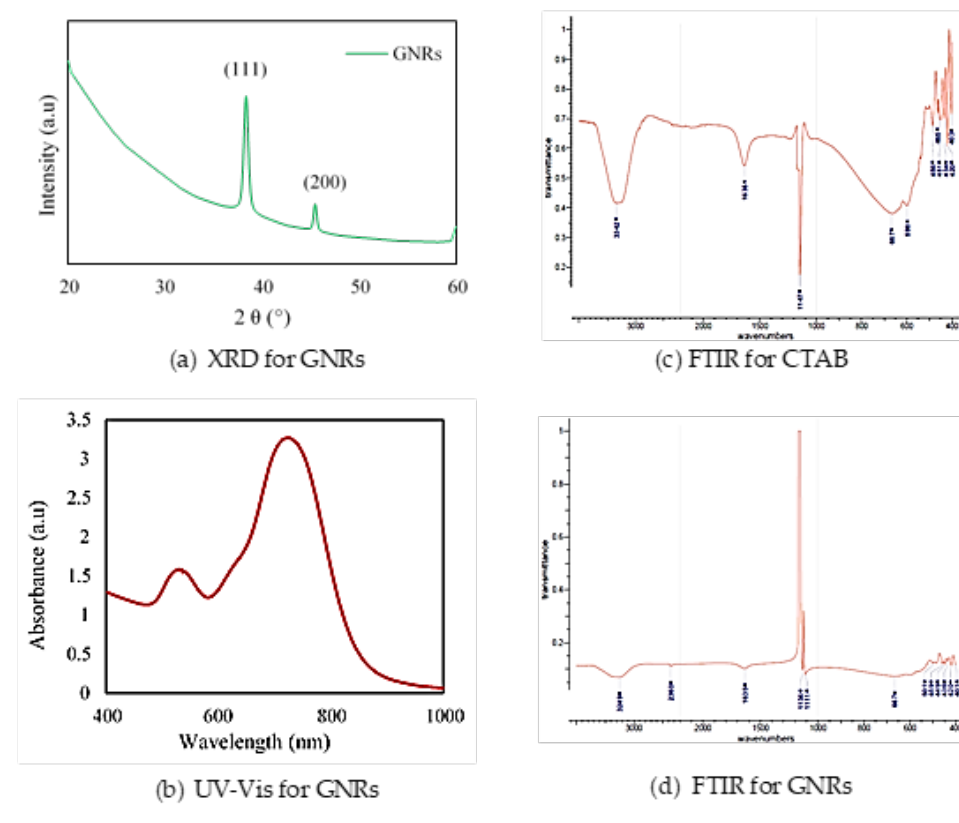


Fig. 6 (a) The structural properties of GNRs; (b), UV-Vis for b) GNRs; (c) FTIR spectrum of CTAB; and (d) GNRs

The optical properties of GNRs were assessed through UV-visible spectroscopy. The absorption spectrum displayed two characteristic plasmonic resonance bands: the transverse surface plasmon resonance (t-SPR) at 521 nm and the longitudinal surface plasmon resonance (l-SPR) at 725 nm, with absorbance values of 1.56 and

3.27 a.u, respectively. These results indicate strong plasmonic activity essential for biomedical and environmental technology applications.

Fourier-transform infrared spectroscopy (FTIR) was used to analyze the functional groups present in the synthesized GNRs. The spectrum of CTAB exhibited sharp absorption peaks at 3342 cm^{-1} , 1635 cm^{-1} , and 1147 cm^{-1} , corresponding to hydroxyl (-OH), carbonyl (C=O), and amide groups. Upon comparing the FTIR spectra of CTAB with that of GNRs, a shift in the hydroxyl group absorption peak was observed, confirming the structural modifications during synthesis. Peaks in the $2200\text{--}3400\text{ cm}^{-1}$ range were attributed to hydroxyl content, while the peak at 1635 cm^{-1} corresponded to amide groups, suggesting interactions with biomolecules that may act as capping agents.

Since CTAB is known to exhibit toxicity at concentrations as low as $10\text{ }\mu\text{M}$, its removal after GNR synthesis was a crucial step. Toxicity assessments indicated that GNRs prepared in this study were free from significant CTAB contamination, making them suitable for biological applications.

3.2 Dengue Vector Control – Larvae and Pupae Treatment using GNRs

Larvaciding and pupiciding have been done under three conditions: no control, temephos, and GNRs for both larvae and pupae. Fig. 7a-c shows the larva conditions after 48 hours of monitoring, while Fig. 7d-f shows the pupae conditions after 48 hours of monitoring. All experiments were run in 200 mL plastic cups containing 100 mL dechlorinated tap water. Different sample conditions were prepared, and 0.1 mL of each preparation was added to the 100 ml water in the cups. The fourth instar larvae and pupae (25/replicate) were put into plastic cups that contained different samples.

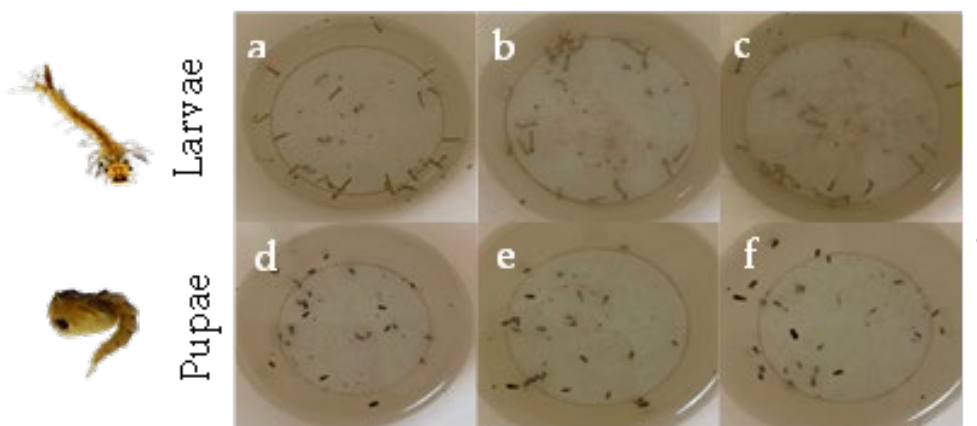


Fig. 7 Larvae and pupae dengue treatment of *Aedes aegypti* using (a); (d) no control; (b)(e) temephos; and (c)(f) GNRs

GNRs interact with the larvae and pupae cuticle through adsorption when applied to breeding sites. The nanoparticles penetrate the exoskeleton or are ingested during the feeding process. The nanoscale dimensions of GNRs lead to physical damage to the cellular membranes. The nanoparticles disrupt enzymatic processes critical for development and survival. Prolonged exposure leads to mortality in mosquito larvae and pupae, reducing the adult mosquito population capable of spreading dengue. The effectiveness of GNRs was tested under controlled laboratory conditions. In summary, there are stages of the process that occur until the mortality of larvae and pupae. Firstly, the electrostatic interaction and binding, in which the positively charged GNRs interact strongly with the negatively charged cell membrane of both larvae and pupae. Due to the electrostatic interaction, the membrane was disrupted, causing leakage of cellular content, leading to cell death. Fig. 8 shows a summary of the method of killing larvae and pupae using GNRs.

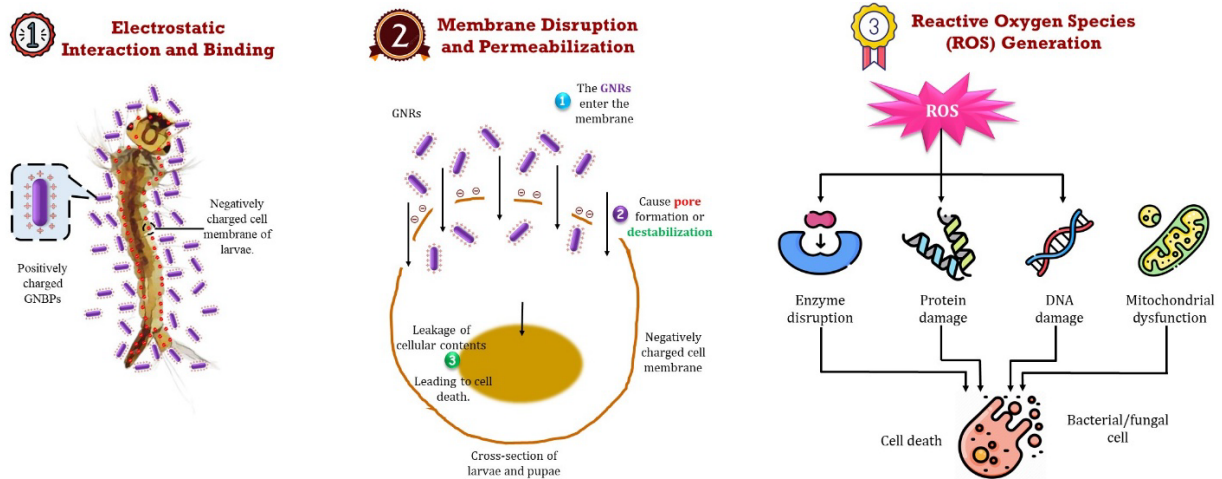


Fig. 8 Method of killing of larvae and pupae using GNRs

Figure 9(a) shows the larvae treated with GNRs, and a noticeable reduction in larval activity is observed, with many larvae appearing dead or inactive. GNRs exhibit significant larvicidal activity, confirming their potential as a nanoparticle-based alternative to chemical larvicides. GNRs caused substantial larval mortality, indicating their potential for use as an alternative larvicide. Besides, the larvae with no control and untreated larvae appear alive and active in the cup, with no visible mortality. This setup serves as a baseline for comparison to measure the effectiveness of treatments. Meanwhile, several larvae exposed to temephos, a commonly used chemical larvicide, appear dead or immobile in the water. This is because temephos is a positive control demonstrating traditional larvicides' efficacy.

Figure 9(b) shows the pupae treated with GNRs. No pupae were dead within 48 hours of treatment. However, the pupae show reduced mobility compared to the control group. GNRs exhibit low pupicidal effects, suggesting they can disrupt pupal development and prevent adult mosquito emergence. GNRs exhibit inherent pupicidal activity, highlighting their potential as nano-based alternatives for controlling *Aedes aegypti* populations. The pupal stage is critical because it directly precedes the adult mosquito stage, which is responsible for spreading diseases like dengue. Disrupting the pupal stage reduces the emergence of adult mosquitoes, thereby breaking the transmission cycle of dengue and other vector-borne diseases. The limited efficacy of temephos on pupae emphasizes the need for alternative strategies, such as nanoparticle-based approaches, to effectively disrupt the mosquito life cycle. Similar to larvae treatment conditions, the pupae appear alive and active in the water under no control, showing no mortality or visible stress. At the same time, pupae exposed to temephos did not show any significant pupal mortality. This observation deviates from its known effectiveness at killing *Aedes aegypti* larvae. Temephos is primarily effective against larvae, not pupae. The results indicate that temephos did not kill the pupae, reinforcing the importance of exploring novel treatments like GNRs for effective dengue vector control.

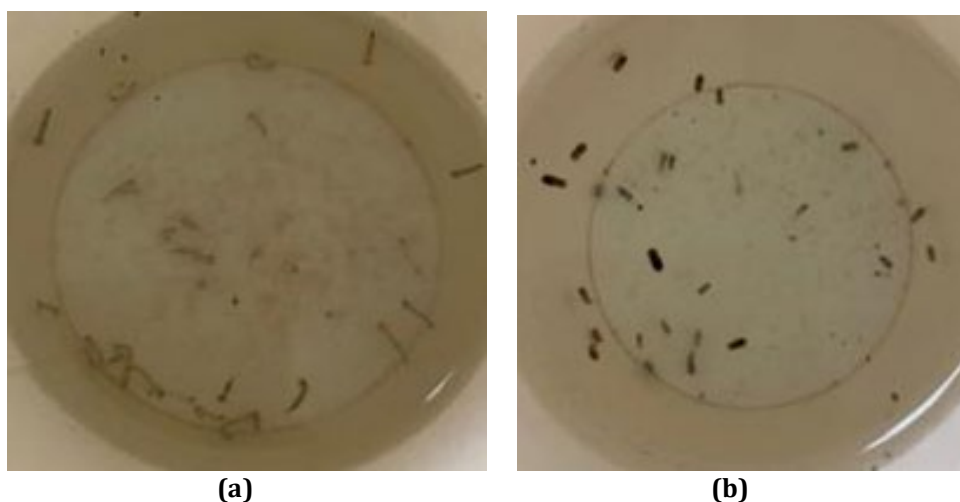


Fig. 9 (a) Larvicide; and (b) Pupicide dengue treatment using GNRs

Fig. 10 shows the mortality rate for larvae and pupae after 5 days of treatment, and the data were tabulated in Table 1. It can be seen that the larvae start to die after 48 hours. From the observation, the mortality rates of larvae after 48, 72, 96, and 120 hours, exposed to GNRs are 10.7 ± 0.6 , 24.0 ± 1.0 , 34.7 ± 0.6 and 48.0 ± 1.0 % respectively. Equation 1 was used to get the mortality rate. Meanwhile, for pupae, the observation shows no dead pupae after 120 hours. However, for a longer period, several pupae die, which might be because of natural causes. The survived pupae are transformed into adult mosquitoes.

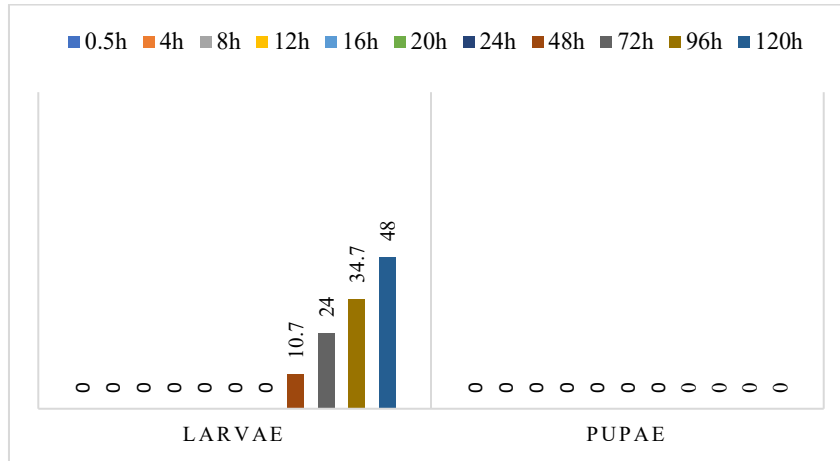


Fig. 10 The mortality rate for larvae and pupae after 5 days of treatment

Table 1 The mortality rate for larvae and pupae after 5 days of treatment

Stage \ Time (h)	0.5	4.0	8.0	12.0	16.0	20.0	24.0	48.0	72.0	96.0	120.0
Larvae	0	0	0	0	0	0	0	10.7 ± 0.60	24.0 ± 1.00	34.7 ± 0.60	48.0 ± 1.00
Pupae	0	0	0	0	0	0	0	0	0	0	0

Next, the dead larvae and pupae treated by GNRs have been observed to check the condition of the samples. Figure 11 shows the morphological image of dead larvae and pupae treated using GNRs. The following observations from Figure 11(a) can be made for head and thorax deformities: the head appears shrunken and wrinkled, indicating structural damage [10]. Deformation around the thoracic region suggests disruption of the larval exoskeleton. Wrinkles and folds on the surface could indicate desiccation or loss of structural integrity, potentially caused by the toxic effects of temephos. For segmental damage, the larval segments exhibit visible disintegration. Surface irregularities, such as cracks or ruptures, can be seen in the body segments. The segmentation looks uneven, which could impact mobility and survival. Then, for overall body deformation, larvae show curvature or bending, suggesting that temephos may have disrupted muscular or neural functions. The smoothness typically seen in untreated larvae is lost, indicating a breakdown of normal cuticular development.

However, when treated at the pupal stage which is a non-feeding stage, the lack of food (tetramin) during laboratory experiments can contribute significantly to pupal mortality. While pupae do not feed, their survival and successful metamorphosis into adults depend on the energy reserves accumulated during the larval stage as shown in Figure 11(b).

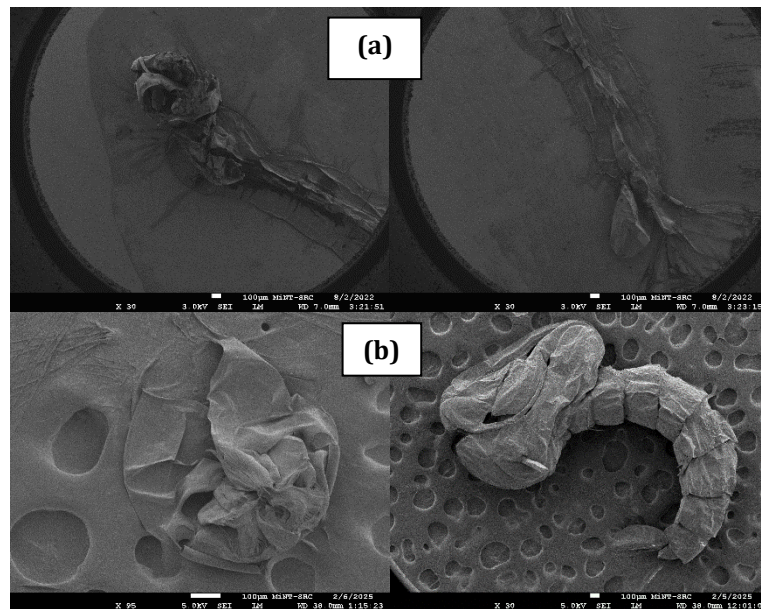


Fig. 11 Morphological deformities induced by the exposure to GNRs of *Aedes aegypti* (a) larvae; and (b) pupae

4. Conclusion

This study demonstrated the potential of GNRs as an alternative vector control strategy against *Aedes aegypti* larvae and pupae. The GNRs were successfully synthesized using the SMGM, with an average length of 72.80 ± 0.53 nm and a width of 16.17 ± 0.19 nm. HR-TEM analysis confirmed their crystalline structure, with a lattice spacing of 0.2008 nm, corresponding to the (200) crystal facets. The optical properties, determined through UV-Vis spectroscopy, exhibited two distinct plasmonic peaks: t-SPR at 521 nm and l-SPR at 725 nm, indicating strong plasmonic activity. XRD analysis further validated the crystalline nature of the synthesized GNRs with diffraction peaks at $2\theta = 38.2^\circ$ (111) plane and $2\theta = 44.5^\circ$ (200) plane.

The larvicidal bioassay results revealed a progressive increase in mortality over time. The mortality rates of fourth-instar *Aedes aegypti* larvae exposed to GNRs were $10.7 \pm 0.6\%$ at 48 hours, $24.0 \pm 1.0\%$ at 72 hours, $34.7 \pm 0.6\%$ at 96 hours, and $48.0 \pm 1.0\%$ at 120 hours, indicating a dose-dependent effect. However, the pupicidal activity was significantly lower, with no mortality observed within the first 120 hours of exposure. Some pupae eventually died after a prolonged period, suggesting that while GNRs may interfere with pupal development, their effectiveness is limited at this stage compared to their impact on larvae.

The morphological analysis of treated larvae confirmed structural deformities, including shrinking of the head, thoracic deformities, and segmentation disintegration, leading to reduced mobility and eventual mortality. The findings suggest that GNRs interact with the larvae through adsorption and ingestion, disrupting physiological processes and causing oxidative stress.

Overall, this study highlights the efficacy of GNRs as a potential nano-based alternative for mosquito control, particularly in targeting *Aedes aegypti* larvae. However, further optimization of nanoparticle concentration, exposure time, and potential combination with other control strategies is necessary to enhance pupicidal effects.

Acknowledgement

This research work was supported financially by the Ministry of Higher Education (MoHE) Malaysia through the Fundamental Research Grant Scheme (FRGS/1/2023/STG05/UTHM/02/3). Special thanks to the International Grant (Vot W024) and Postgraduate Research Grant (GPPS) (Vot H690) for partially supporting this research. The authors thank Microelectronics & Nanotechnology-Shamsuddin Research Centre (MiNT-SRC), Universiti Tun Hussein Onn Malaysia, for the related facilities.

Conflict of Interest

Marlia Morsin and Rahmat Sanudin are Universiti Tun Hussien Onn Malaysia academicians. Nur Liyana Razali is a postgraduate student at Universiti Tun Hussien Onn Malaysia. Nur Zehan An'nisa is an engineer and graduate Master's student from UTHM. Suratun Nafisah is a lecturer at Institut Teknologi Sumatera (ITERA).

Ethical Approval

This work is original and has not been published and submitted simultaneously for publication elsewhere.

Author Contribution

The authors confirm contribution to the paper as follows: **study conception and design:** Marlia Morsin, Nur Liyana Razali and Suratun Nafisah; **data collection:** Nur Liyana Razali; **analysis and interpretation of results:** Marlia Morsin, Nur Liyana Razali, Rahmat Sanudin and Suratun Nafisah; **draft manuscript preparation:** Nur Liyana Razali, Nur Zehan An'nisa Md Shah, Marlia Morsin and Rahmat Sanudin. All authors reviewed the results and approved the final version of the manuscript.

References

- [1] World Health Organization, "Dengue and Severe Dengue," World Health Organization. Accessed: Feb. 06, 2025. [Online]. Available: <https://www.who.int/news-room/fact-sheets/detail/dengue-and-severe-dengue>
- [2] K. Mysore *et al.*, "Development of a controlled-release mosquito RNAi yeast larvicide suitable for the sustained control of large water storage containers," *Sci. Rep.*, vol. 14, no. 1, pp. 1–13, 2024, doi: 10.1038/s41598-024-81800-5.
- [3] S. J. Gan *et al.*, "Dengue fever and insecticide resistance in Aedes mosquitoes in Southeast Asia: a review," *Parasites and Vectors*, vol. 14, no. 1, pp. 1–19, 2021, doi: 10.1186/s13071-021-04785-4.
- [4] J. A. S. Bonds, "Ultra-low-volume space sprays in mosquito control: A critical review," Jun. 2012. doi: 10.1111/j.1365-2915.2011.00992.x.
- [5] G. Gupta *et al.*, "DDPM: A Dengue Disease Prediction and Diagnosis Model Using Sentiment Analysis and Machine Learning Algorithms," *Diagnostics*, vol. 13, no. 6, 2023, doi: 10.3390/diagnostics13061093.
- [6] J. Thelma and C. Balasubramanian, "Ovicidal, larvicidal and pupicidal efficacy of silver nanoparticles synthesized by Bacillus marisflavi against the chosen mosquito species," *PLoS One*, vol. 16, no. 12, December, pp. 1–19, 2021, doi: 10.1371/journal.pone.0260253.
- [7] N. Chimkhan, S. N. R. Thammasittirong, S. Roytrakul, S. Krobthong, and A. Thammasittirong, "Proteomic Response of Aedes aegypti Larvae to Silver/Silver Chloride Nanoparticles Synthesized Using Bacillus thuringiensis subsp. israelensis Metabolites," *Insects*, vol. 13, no. 7, 2022, doi: 10.3390/insects13070641.
- [8] M. L. Warbanski, P. Marques, T. C. Frauendorf, D. A. T. Phillip, and R. W. El-Sabaawi, "Implications of guppy (Poecilia reticulata) life-history phenotype for mosquito control," *Ecol. Evol.*, vol. 7, no. 10, pp. 3324–3334, 2017, doi: 10.1002/ece3.2666.
- [9] C. D. Chen *et al.*, "Biting behavior of Malaysian mosquitoes, Aedes albopictus Skuse, Armigeres kesseli Ramalingam, Culex quinquefasciatus Say, and Culex vishnui Theobald obtained from urban residential areas in Kuala Lumpur," *Asian Biomed.*, vol. 8, no. 3, pp. 315–321, 2014, doi: 10.5372/1905-7415.0803.295.
- [10] K. Sivabalakrishnan *et al.*, "Resistance to the larvicide temephos and altered egg and larval surfaces characterize salinity-tolerant Aedes aegypti," *Sci. Rep.*, vol. 13, no. 1, pp. 1–12, 2023, doi: 10.1038/s41598-023-35128-1.
- [11] J. M. Wong *et al.*, "Dengue: A Growing Problem With New Interventions," *Pediatrics*, vol. 149, no. 6, 2022, doi: 10.1542/peds.2021-055522.
- [12] S. Renganathan *et al.*, "Silver nanoparticle synthesis from carica papaya and virtual screening for anti-dengue activity using molecular docking," *Mater. Res. Express*, vol. 6, no. 3, pp. 1–12, Mar. 2019, doi: 10.1088/2053-1591/aaf6fb.
- [13] M. Kus-lińskiewicz, P. Fickers, and I. Ben Tahar, "Biocompatibility and cytotoxicity of gold nanoparticles: Recent advances in methodologies and regulations," *Int. J. Mol. Sci.*, vol. 22, no. 20, 2021, doi: 10.3390/ijms222010952.
- [14] J. Georgeous, N. AlSawafah, W. H. Abuwatfa, and G. A. Hussein, "Review of Gold Nanoparticles: Synthesis, Properties, Shapes, Cellular Uptake, Targeting, Release Mechanisms and Applications in Drug Delivery and Therapy," *Pharmaceutics*, vol. 16, no. 10, 2024, doi: 10.3390/pharmaceutics16101332.
- [15] S. Nafisah *et al.*, "Improved Sensitivity and Selectivity of Direct Localized Surface Plasmon Resonance Sensor Using Gold Nanobipyramids for Glyphosate Detection," *IEEE Sens. J.*, vol. 20, no. 5, pp. 2378–2389, 2020, doi: 10.1109/JSEN.2019.2953928.

- [16] M. Morsin, A. A. Umar, M. M. Salleh, and B. Yeop, "High Sensitivity Localized Surface Plasmon Resonance Sensor of Gold Nanoparticles : Surface Density Effect for Detection of Boric Acid," in *International Conference on Semiconductor Electronics*, 2012, pp. 352–356.
- [17] N. Z. A. Md Shah, M. Morsin, R. Sanudin, N. L. Razali, S. Nafisah, and C. F. Soon, "Effects of Growth Solutions Ageing Time to the Formation of Gold Nanorods via Two-Step Approach for Plasmonic Applications," *Plasmonics*, vol. 15, no. 4, pp. 923–932, 2020, doi: 10.1007/s11468-019-01098-2.
- [18] N. S *et al.*, "Biogenic Synthesis of Silver Nanoparticles and Valuation of their Antimicrobial Activity against Dengue Larvae," *J. Plant Pathol. Microbiol.*, vol. 8, no. 8, pp. 1–5, 2017, doi: 10.4172/2157-7471.1000418.
- [19] W. Journal and O. F. Pharmaceutical, "Larvicidal nanoparticle to control aedes aegypti," vol. 8, no. 8, pp. 38–43, 2022.
- [20] M. Yazhini Prabha, B. Vaseeharan, A. Sonawane, and A. Behera, "In vitro and In vivo toxicity assessment of phytofabricated ZnO nanoparticles showing bacteriostatic effect and larvicidal efficacy against *Culex quinquefasciatus*," *J. Photochem. Photobiol. B Biol.*, vol. 192, no. January, pp. 158–169, 2019, doi: 10.1016/j.jphotobiol.2019.01.014.
- [21] K. Dass, "Green Synthesis of Silver Nanoparticles for Mosquito Control : A Review of Larvicidal Activity from Plant Extracts," no. December, 2024, doi: 10.56557/upjoz/2024/v45i224677.
- [22] H. P. Piepho *et al.*, "Efficacy assessment in crop protection: a tutorial on the use of Abbott's formula," *J. Plant Dis. Prot.*, vol. 131, no. 6, pp. 2139–2160, 2024, doi: 10.1007/s41348-024-00968-0.